Journal of Electroanalytical Chemistry 986 (2025) 119081

Contents lists available at ScienceDirect

Journal of Electroanalytical Chemistry

journal homepage: www.elsevier.com/locate/jelechem

Unveiling novel capacity (electro)recovery for Chloranilate-based alkaline redox flow batteries

Ali Tuna [a,b,*,1], Vahid Abbasi [a,1], Carita Kvarnström [b], Pekka Peljo [a,*]

[a] University of Turku, Division of Materials Engineering, Vesilinnantie 5, FI-20014 Turku, Finland
[b] University of Turku, Department of Chemistry, Henrikinkatu 2, FI-20014 Turku, Finland

ARTICLE INFO

Keywords:
Chloranilic acid
Alkaline
Flow battery
(electro)recovery

ABSTRACT

This study monitors a two-electron chloranilate-ferrocyanide redox flow battery system in alkaline media at 1.1 V, focusing on capacity recovery during charge-discharge operations. Capacity decay is relatively stabilized and restored via electrochemical oxidation process at certain steps. Different concentrations and cycle performances are also tested.

1. Introduction

Energy storage is important in connecting variable renewable energy sources with energy consumption. For renewable energy to be widely used, affordable and efficient storage options need to have a lasting impact [1–3]. Due to the instability of renewable energy, reliable storage systems are needed to store additional energy during peak production periods and to regularly distribute on demand. Redox flow batteries (RFBs) are electrochemical energy storage systems that unlike traditional batteries, store energy in electrolyte solutions, allowing independent control of energy and power [4–7].

Organic flow batteries (ORFBs) offer several advantages compared to inorganic redox flow battery systems. Several organic compounds are used as redox mediators (active materials) that can be tuned to increase electrical power and improve overall performance [1,2,6–8]. ORFBs generally have high capacity [16], improved efficiency [17,18], and low cost due to the availability and accessibility of biological materials such as plants extractions, etc. In addition, Aqueous organic redox flow batteries can be considered safe and environmentally friendly electrochemical energy storage systems due to their use of non-toxic, abundant organic materials and water-based electrolytes, which relatively minimize the risk of flammability and environmental contamination. The flexible molecular structure allows for better tuning of the battery's components, resulting in higher energy and longer life time [1,4,7,9].

Quinone-based redox flow batteries are a promising new system in energy storage technology, using organic compounds to store and release electrical energy efficiently by reducing one or two electrons depending on the chemical environment. Various types of quinones, such as benzoquinones [10], naphthoquinones [11,12], anthraquinones [13–15], have been studied for the construction of quinone-based redox flow batteries (Fig. 1).

The inherent advantages of quinones, such as their abundance, low cost, and environmental compatibility, make them an attractive choice for redox flow batteries. The ability to tailor quinone structures further enhances the tunability of these batteries, allowing to optimize performance characteristics such as energy density, cycling stability, and efficiency [10,11,13].

2,5-dihydroxy-1,4-benzoquinone-based redox flow battery system was previously studied [10], however commercial availability is limited due to high prices. The chlorinated derivative of 2,5-dihydroxy-1,4-benzoquinone, which is also called, chloroanilic acid is economically favourable (almost ten-times cheaper than its non-chlorinated derivative), and higly soluble in aqueous Li^+ media. In our studies, we have aimed to use chloroanilic acid in Li^+ media and battery performance of a novel redox flow battery system were optimized for the first time (See Scheme 1).

2. Results and discussion

The solubility tests for chloranilic acid were made in different 1 M alkaline electrolytes (LiOH, NaOH, KOH, NH_4OH) and neutral pH electrolytes (LiCl, NaCl, KCl, NH_4Cl) to be found that LiOH gave the

* Corresponding authors at: University of Turku, Division of Materials Engineering, Vesilinnantie 5, FI-20014 Turku, Finland.
E-mail addresses: ali.tuna@utu.fi (A. Tuna), pekka.peljo@utu.fi (P. Peljo).
[1] A. T. and V. A. contributed equally to this work

https://doi.org/10.1016/j.jelechem.2025.119081
Received 26 December 2024; Received in revised form 2 March 2025; Accepted 14 March 2025
Available online 27 March 2025

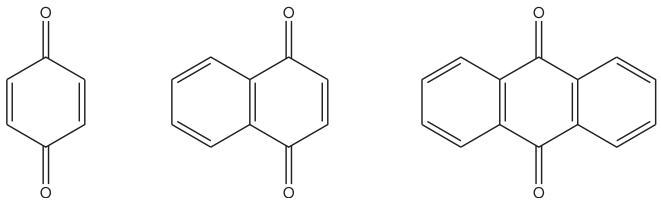

Fig. 1. The simple chemical structures of 1,4-benzoquionone (left), 1,4-naphthaquinone (middle), and 9,10-anthraquionone (right).

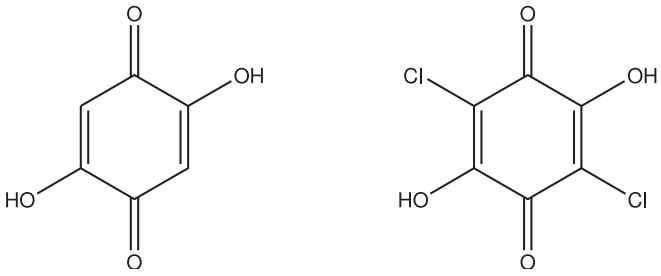

Scheme 1. The chemical structures of 2,5-dihydroxy-1,4-benzoquinone (left) and chloranilic acid (right)

highest solubility, the order to be found LiOH (280 mM) > > LiCl (~100 mM) > NH_4OH (70 mM) > NaOH (40 mM) > > KOH (~10 mM) > > NH_4Cl > NaCl > KCl, respectively, and reversible redox peak formation at room temperature. The combined cyclic voltammograms of lithium chloranilate and lithium ferrocyanide chloranilic acid in 1 M LiOH were shown in Fig. 2.

Due to the high cation selectivity and good ionic conductivity, Nafion 212 was decided to be used in the battery setup. Additionally, commercial sodium and potassium salts of ferrocyanide were found to be unsuitable for use due to low solubility of redox active negolyte material, therefore lithium ferrocyanide (LiHCF) salt was prepared to be used in the posolyte side of the battery in order to avoid any negative impact of counter ion as low solubility of chloranilate in Na^+ and K^+ containing alkaline media. Cyclic voltammogram of chloranilate in the presence of Li^+ was run in the presence of lithium ferrocyanide, which is

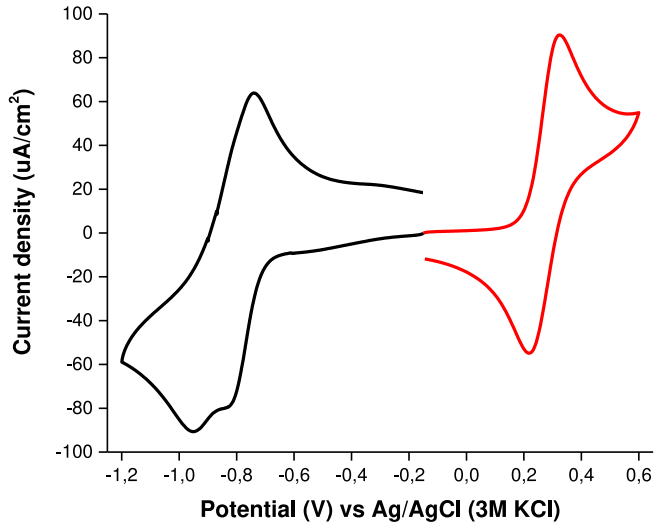

Fig. 2. Cyclic voltammograms of the lithium chloranilate (left, black) as negolyte for the battery and lithium ferrocyanide (right, red) as posolyte side of the system in 1 M LiOH with a 50 mV/s scan rate. (For interpretation of the references to color in this figure legend, the reader is referred to the web version of this article.)

a suitable posolyte. These two redox molecules (posolyte and negolyte) did not show any unusual interactions to each other and it was concluded that they could be suitable together under these conditions, see Fig. 2.

Following the obtained reversible cyclic voltammograms of lithium chloranilate and lithium ferrocyanide battery setup, the experimental battery studies were performed. A two-electron reversible reduction in this system was observed with peak potentials of approximately −0.89 V vs Ag/AgCl. From the dQ/dV profile determined (Fig. S5) from the battery software it was observed that two electrons are involved for redox processes. According to the observed results in this profile, two-steps redox reactions occur in the 1.1 V battery preserved during charge-discharges in the presence of Li^+ containing alkaline media have been proven.

The installed battery system setup was monitored under various conditions with different charge and discharge parameters such as voltage and currents, and as a result, capacity decay was observed (Fig. 3). The decay comes from dimerization of charged species as described in Eq. 1–4. that are not electroactive after dimerization [22,24]. Higher concentration of chloranilate results in faster dimerization rate as the charged species can find and make the reaction easier. The effect of increasing concentration is shown in Fig. 3.

All the assembled batteries in this paper have used the same electrolyte in Negolyte and Posolyte to prevent crossover or osmosis pressure. A high concentration of LiHCF was used in the posolyte to have the lithium chloranilate (negolyte) as limiting factor to investigate, tests have been measured in glovebox (N_2 environment).

In order to restore the capacity back by recovering the monomers from the dimers, first achieved by chemical oxidation (see Eq. 5) by using air bubbling through the solution until the color changes from light yellow to purple as original chloranilate anion's color in alkaline media. The capacity recovery is shown in Fig. 4. The coulombic efficiency in the Fig. 4 for the recovery step is 0 % because the air bubbling was done when battery was fully charged. Thus, the battery could be discharged by air at the same time as electrorecovery (Scheme 2). Quinone molecules in the flow battery have the capacity to charge and discharge 2 electrons but practically just 60–90 % of the 2 e^- capacity achieved [14,19–21]. In our system, the capacity after recovery increased in this case and the root of this increasement is by introducing the O_2 to the solution, the media is getting alkaline and the redox active material works better in higher pH, as this is discussed further.

Then, the battery tests were reprogrammed to add an additional step and after certain cycles, it was formed electrochemically without the contribution of an external oxidative substance. Similar recovery steps

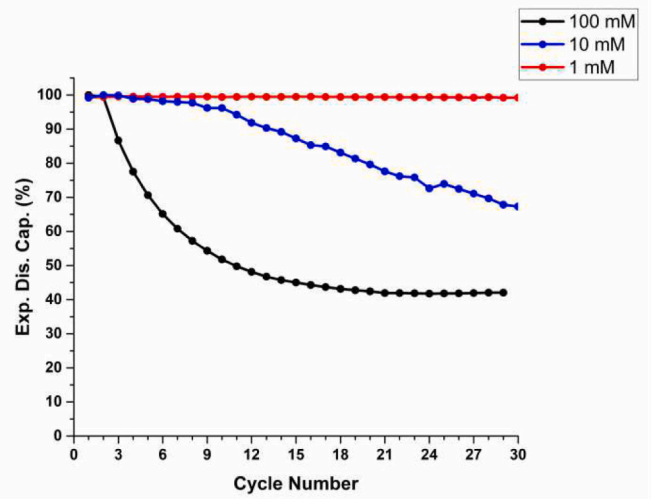

Fig. 3. The batteries with different concentration of lithium chloranilate (Negolyte) vs LiHCF (Posolyte in excess) in 1 M LiOH.

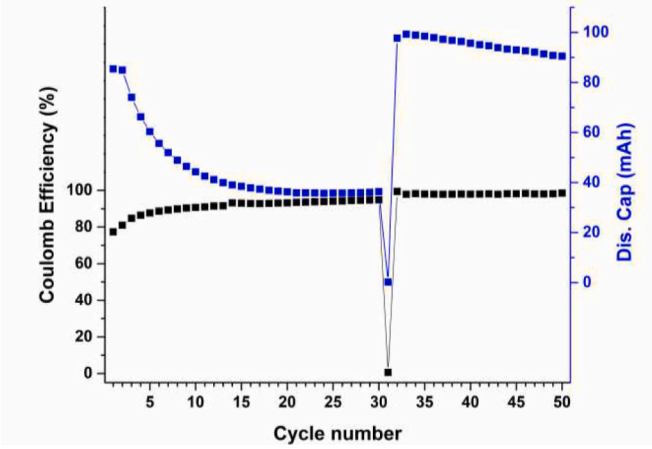

Fig. 4. The capacity recovery using bubbling air into the solution.

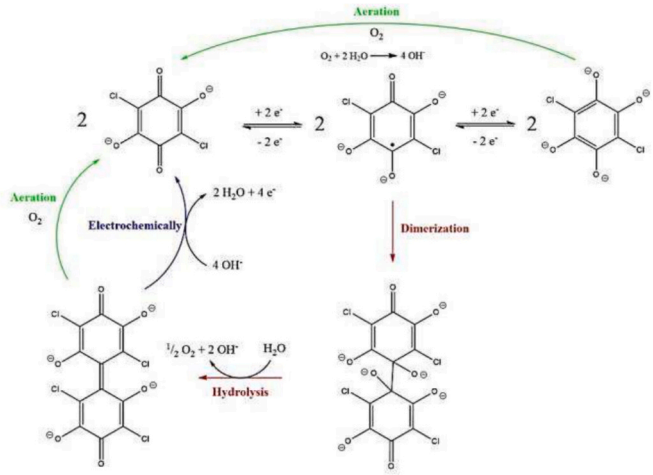

Scheme 2. The proposed mechanism of chloranilate two-electron reduction and NMR and UV–vis assisted structural change to dimeric specie formation and its electrochemical oxidation to chloranilate in alkaline media

were applied in literature [22–24]. Thus, by transforming the redox-inactive structure that causes capacity decay into the starting material, capacity loss was prevented and the battery's lifetime was tried to be partially extended for longer and better applications. This step can be seen from the Fig. 5, which the cycle after the recovery takes more time to charge and discharge, basically showing more capacity.

At the recovery step, the battery should be discharged (at this step there are the initial molecules and the formed dimers), by setting current to a lower value (2 mA/cm [2]) and going to negative potentials we are taking electrons from the negolyte side. The reaction in Eq. 4 starts happening at −0.5 V from the battery potential which is 0.2 V vs SHE for the negolyte. The positive value of this reaction shows the favourability of the reaction and confirms the oxygen recovery can happen without applying any potential. This step is usually done with applying lower current to give opportunity to all the dimers to be oxidized to first monomers, and when the formed dimers in the Eq. 4 converted to the initial monomers, the electrorecovery curve goes down. Here is the point that it should be stopped to avoid side reactions.

$$C_6Cl_2O_4^{2-} + e^- \rightarrow C_6Cl_2O_4^{3\bullet-} \quad (1)$$

$$C_6Cl_2O_4^{3\bullet-} + e^- \rightarrow C_6Cl_2O_4^{4-} \quad (2)$$

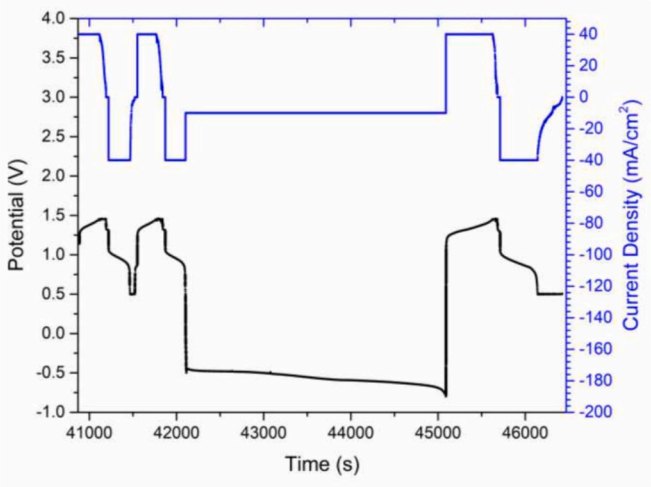

Fig. 5. Electro-capacity recovery step (extra-discharging the battery) which breaks the dimer bond.

$$2\,C_6Cl_2O_4^{3-} + H_2O \rightarrow C_{12}Cl_4O_6^{4-} + 2\,OH^- + \frac{1}{2}O_2 \quad (3)$$

$$C_{12}Cl_4O_6^{4-} + 4\,OH^- \rightarrow 2\,C_6Cl_2O_4^{2-} + 2H_2O + 4\,e^- \quad (4)$$

As a first step, two-negatively charged chloranilate ($C_6Cl_2O_4^{2-}$) can go under one-electron reversible reduction to form a three-negatively charged radical specie of chloranilate as a semi-quinone structure ($C_6Cl_2O_4^{\bullet 3-}$) at E = −0.84 V (Eq. 1) vs Ag/AgCl in 3 M KCl. Then it can be one-electron reversible reduction to form a four-negatively charged chloranilate as a quinone structure ($C_6Cl_2O_4^{4-}$) at E = − 0.97 V (Eq. 2) vs Ag/AgCl in 3 M KCl. The formed three-negatively charged chloranilate radical anion specie can be irreversibly form a four-negatively charged dimeric structure of a quinone ($C_{12}Cl_4O_6^{4-}$) in alkaline condition (Eq. 3). During this formation, pH is increased due to consumed H_2O molecules and formed OH^- ions. Such formation can be seen from the color change of green to yellowish. This dimer formation can be also explanation of the capacity-fade to form a new structure which has different potential to act electrochemically. The formed dimeric structure can be electrochemically oxidized back to two-negatively charged chloranilate at E = −0.5 V (Eq. 4). The formed dimeric structure can be alternatively oxidized by air-purging through the solution outside was tried and detected the color change from yellow to purple as oxygen (O_2) can decompose to dimer structure to form two-negatively charged chloranilate (Eq. 5).

$$C_{12}Cl_4O_6^{4-} + O_2 \rightarrow 2\,C_6Cl_2O_4^{2-} \quad (5)$$

The electrochemical process and molecular changes can be also illustrated with molecular drawing as below (Scheme 2).

In the first few cycles of a redox flow battery, the coulombic efficiency naturally improves as the system settles in. The reason is that however the solution is bubbled with N_2 and the test is done in the glovebox, but still there is a bit oxygen left in the solution which goes into the irreversible reaction with the charged redox active material. But over time, it is consumed and the system is stabilized. In lower concentration test (Fig. 6. top), this stabilization takes more time and the stabilization process affects more cycles. In Fig. 6. middle and bottom graphs, there are cycles which the coulombic efficiency exceeding 100 % during the recovery step. This indicates that more electrons are consumed during the discharge process than were supplied during charging. This occurs because the recovery step, which takes place after the main discharge, is also classified as part of the discharge process but happens at negative potentials.

As a result, additional electrons are transferred beyond the initial

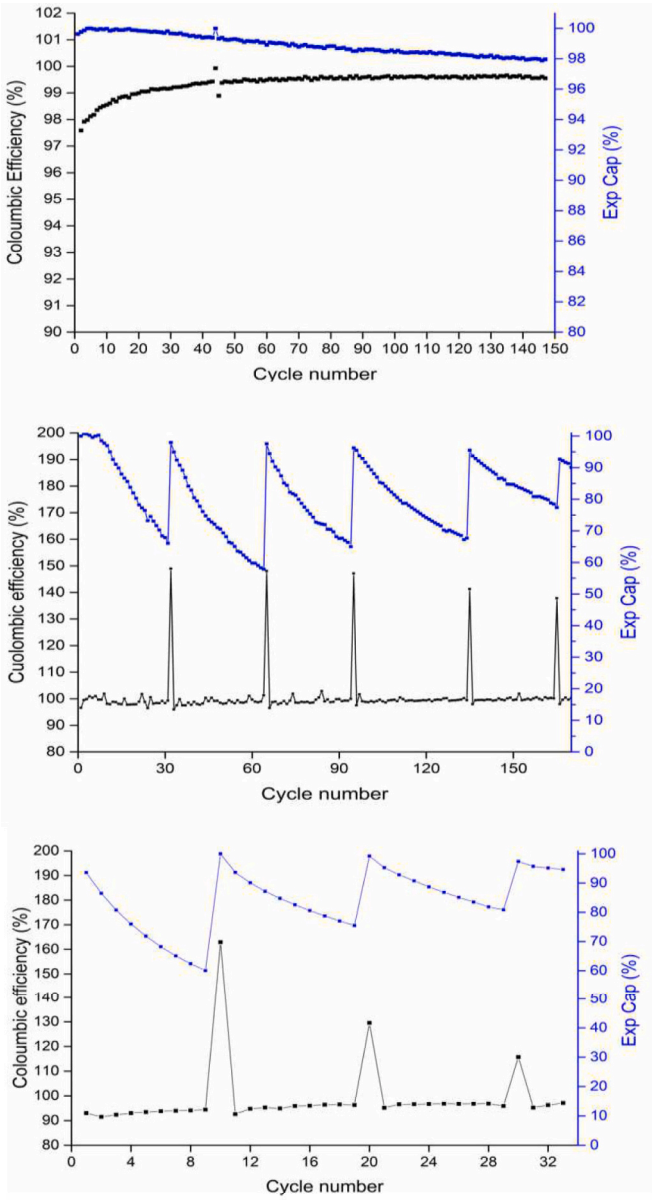

Fig. 6. Electro-capacity recovery for different concentration of lithium chloranilate in 1 M LiOH (negolyte); 1 mM (top), 10 mM (middle) and 100 mM (bottom) vs LiHCF (posolyte) in excess.

charge input, leading to an apparent coulombic efficiency greater than 100 %. This effect arises from the nature of the recovery step, where the dimer participates in redox reactions, contributing to extra electron flow during discharge to become the starting material.

Fig. 6 shows the effect of the recovery step for different concentrations of lithium chloranilate. The battery with low concentration of 1 mM does not need the recovery step as it the dimerization rate in the low concentration is negligible and if we apply the recovery step to the solution, not only the capacity does not get back, but also, solution will lose the active materials as high potential can oxidize the monomers destructively by side reactions. as shown in Fig. 6 middle and bottom, by increasing the concentration the decay is stronger and the recovery should be done sooner. Basically, by losing 60–70 % of the capacity one electrorecovery step has been applied. This capacity fade for 10 mM is each 30 cycles and for 100 mM is every 10 cycles. And the cycle numbers for each recovery stayed constant to observe the changes from the next recoveries.

In next recoveries the coulombic efficiency of the recovery steps decreased because there is less dimerization and the rate of dimerization is decreased. This happens because 4 OH^- molecule are consumed in each recovery step for each dimer (as shown in Eq. 4) and the solution pH is getting lower and lower by each step of recovery. By decreasing the pH, the dimerization rate gets lower and battery works better but in low pH applying the recovery step is not possible.

In order to have lower dimerization rate, optimization of the pH has been done, shown in Fig. 7. The black points at the 0.5 M and 0.3 M of LiOH electrolyte are the applied recovery steps which failed because there is no enough OH^- in the media to involve to the recovery step. The pourbaix diagram (Fig. S8) approves the potential of the lithium chloranilte is not changing by changing the pH.

Considering all experimental results together with ^{13}C NMR and UV–vis spectra, the mechanistic approach was concluded the formation of dimer started from $1e^-$ reduction of chloranilate followed by hydrolysis and it can be either recovered by molecular O2 and electrochemically discharging at negative potentials. The more detailed spectral data can be seen in ESI.

3. Conclusion

As a first time, lithium chloranilate was proposed to be used in redox flow batteries as a cost-friendly negolyte material. Lithium chloranilate was electrochemically investigated. Capacity loss during battery measurements was prevented first using molecular oxygen and then it was replaced by electrochemical oxidation to disform the dimerized molecule which yielded in the capacity decay was restored as it re-oxidized to dianionic chloranilate molecules. Furthermore, the various conditions were also studied to understand how this system work properly. The effects of concentration and pH on the capacity loss occurring during all battery operations were also discussed and investigated with various measurements. The capacity recovery can be done by electrochemically in certain conditions. As higher pH makes, compound more efficient and more capacity is achieved. It was shown that chloranilate-based redox flow batteries can applicable due to its cyclability and reversibility.

Notes and references

We would like to thank to European Research Council (Bi3Boost-FlowBat project, agreement no. 950038), and special thanks to Gabriel Gonzalez, Eduardo Martinez-Gonzalez and Sami Vuori for scientific discussions.

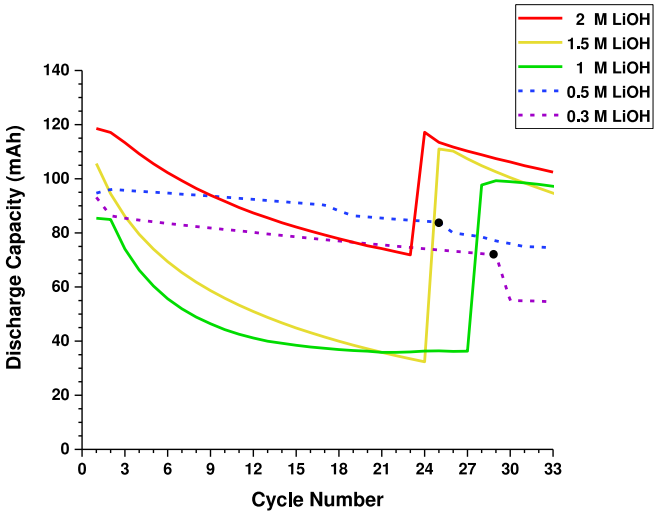

Fig. 7. The electrochemical recovery tests for 100 mM LiChA in different LiOH concentrations.

CRediT authorship contribution statement

Ali Tuna: Writing – review & editing, Writing – original draft, Visualization, Validation, Methodology, Investigation, Formal analysis, Data curation, Conceptualization. **Vahid Abbasi:** Writing – review & editing, Writing – original draft, Visualization, Validation, Methodology, Investigation, Formal analysis, Data curation. **Carita Kvarnström:** Writing – review & editing, Supervision, Resources. **Pekka Peljo:** Writing – review & editing, Writing – original draft, Validation, Supervision, Resources, Conceptualization.

Declaration of competing interest

The authors declare that they have no known competing financial interests or personal relationships that could have appeared to influence the work reported in this paper.

Appendix A. Supplementary data

Supplementary data to this article can be found online at https://doi.org/10.1016/j.jelechem.2025.119081.

Data availability

The data supporting this article have been included as part of the ESI.

References

[1] X. Fang, A.T. Cavazos, Z. Li, C. Li, J. Xie, S.R. Wassall, L. Zhang, X. Wei, Chem. Commun. 58 (2022) 13226–13229.
[2] T.P. Vaid, M.S. Sanford, Chem. Commun. 55 (2019) 11037–11040.
[3] A.N. Colli, P. Peljo, H.H. Girault, Chem. Commun. 52 (2016) 14039–14042.
[4] B. Hu, Y. Tang, J. Luo, G. Grove, Y. Guo, T.L. Liu, Chem. Commun. 54 (2018) 6871–6874.
[5] Z. Yuan, H. Zhang, X. Li, Chem. Commun. 54 (2018) 7570–7588.
[6] E.I. Romadina, D.S. Komarov, K.J. Stevenson, P.A. Troshin, Chem. Commun. 57 (2021) 2986–2989.
[7] O. Simoska, Z. Rhodes, E. Carroll, K.N. Petrosky, S.D. Minteer, Chem. Commun. 59 (2023) 2142–2145.
[8] S. Schaltin, Y. Li, N.R. Brooks, J. Sniekers, I.F.J. Vankelecom, K. Binnemans, J. Fransaer, Chem. Commun. 52 (2016) 414–417.
[9] T. Murata, M. Hamasaki, Y. Morita, Chem. Commun. 60 (2023) 878–880.
[10] Z. Yang, L. Tong, D.P. Tabor, E.S. Beh, M.A. Goulet, D. De Porcellinis, A. Aspuru-Guzik, R.G. Gordon, M.J. Aziz, Adv. Energy Mater. 8 (2018) 1702056.
[11] P. Hu, H. Lan, X. Wang, Y. Yang, X. Liu, H. Wang, L. Guo, Energy Storage Mater 19 (2019) 62–68.
[12] L. Tong, M.A. Goulet, D.P. Tabor, E.F. Kerr, D. De Porcellinis, E.M. Fell, A. Aspuru-Guzik, R.G. Gordon, M.J. Aziz, ACS Energy Lett. 4 (2019) 1880–1887.
[13] Kaixiang Lin, Qing Chen, Michael R. Gerhardt, Michael J. Aziz, Science 349 (2015) 1529–1532.
[14] B. Yang, A. Murali, A. Nirmalchandar, B. Jayathilake, G.K.S. Prakash, S. R. Narayanan, J. Electrochem. Soc. 167 (2020) 060520.
[15] S. Jin, Y. Jing, D.G. Kwabi, Y. Ji, L. Tong, D. De Porcellinis, M.A. Goulet, D. A. Pollack, R.G. Gordon, M.J. Aziz, ACS Energy Lett 4 (2019) 1342–1348.
[16] Z. Xiang, T. Ren, M. Huang, W. Li, L. Wang, K. Wan, Z. Fu, Z. Liang, Angew. Chem. Int. Ed. 64 (2025) e202416184.
[17] X. Yuan, M. Huang, Z. Liang, Int. J. Heat Mass Transf. 205 (2023) 123924.
[18] W. Li, S. Liao, Z. Xiang, M. Huang, Z. Fu, L. Li, Z. Liang, Chem. Eng. Sci. 270 (2023) 118534.
[19] P. Symons, Curr. Opin. Electrochem. 29 (2021) 100759.
[20] Y. Jing, M. Wu, A.A. Wong, E.M. Fell, S. Jin, D.A. Pollack, E.F. Kerr, R.G. Gordon, M.J. Aziz, Green Chem. 22 (2020) 6084–6092.
[21] S. Jin, Y. Jing, D.G. Kwabi, Y. Ji, L. Tong, D. De Porcellinis, M.-A. Goulet, D. A. Pollack, R.G. Gordon, M.J. Aziz, ACS Energy Lett. 4 (6) (2019) 1342–1348.
[22] Y. Jing, E.W. Zhao, M.-A. Goulet, M. Bahari, E.M. Fell, S. Jin, A. Davoodi, E. Jónsson, M. Wu, C.P. Grey, R.G. Gordon, M.J. Aziz, Nat. Chem. 14 (2022) 1103–1109.
[23] M. Bahari, Y. Jing, S. Jin, M.-A. Goulet, T. Tsukamoto, R.G. Gordon, M.J. Aziz, A.C. S. Appl, Mater, Interfaces 16 (39) (2024) 52144–52152.
[24] K. Amini, E.F. Kerr, T.Y. George, A.M. Alfaraidi, Y. Jing, T. Tsukamoto, R. G. Gordon, M.J. Aziz, Adv. Funct. Mater. 33 (2023) 2211338.